BIOCHEMISTRY
including biophysical chemistry & molecular biology

ARTICLE

pubs.acs.org/biochemistry

Differential and Synergistic Effects of Epidermal Growth Factor Receptor Antibodies on Unliganded ErbB Dimers and Oligomers

Noga Kozer,[†,§] Marcus P. Kelly,[†] Suzanne Orchard,[†] Antony W. Burgess,[†] Andrew M. Scott,[*,‡] and Andrew H. A. Clayton[*,†,§]

[†]Ludwig Institute for Cancer Research, Melbourne-Parkville Branch, Royal Melbourne Hospital, Victoria 3050, Australia

[‡]Ludwig Institute for Cancer Research, Melbourne-Austin Branch, Austin Hospital, Studley Road, Heidelberg, Victoria 3084, Australia

[§]Centre for Micro-Photonics, Faculty of Engineering and Industrial Sciences, Swinburne University of Technology, Hawthorn, Victoria 3122, Australia

Supporting Information

ABSTRACT: Antibodies directed against the epidermal growth factor receptor (EGFR) offer a potentially powerful therapeutic approach against cancers driven by the EGFR pathway. EGFR antibodies are believed to halt cell surface activation by blocking ligand-induced receptor tyrosine kinase activation, i.e., ligand binding, a change in conformation, or the monomer−dimer transition. In this work, we demonstrate that wild-type EGFR and the truncated de2−7-EGFR (tumor-associated mutant) formed unliganded homo-oligomers and examined the effects of two clinically relevant antibodies on the conformation and quaternary state of these ligand-free EGFR oligomers on the surface of cells. The EGFR antibodies were mAb528, a ligand-blocking antibody that binds domain III, and mAb806, a conformationally sensitive antibody that binds near the dimer interface in domain II. We used a model cellular system, BaF/3 cells, with GFP-tagged receptors in the absence of interference from secreted ligands or other erbB receptor members. Different antibody-mediated effects (conformational transition, receptor cross-linking, or receptor dissociation) were distinguished by combining two complementary biophysical techniques: image correlation spectroscopy (submicrometer scale clustering) and homo-Forster resonance energy transfer (association and/or conformation on a 1−10 nm scale). mAb528 cross-linked EGFR into an inactive EGFR dimer of dimers but had no effect when added to de2−7-EGFR oligomers. mAb806 had a minor effect on EGFR dimers as expected from its poor binding to a conformationally shielded epitope on wtEGFR but bound de2−7-EGFR oligomers, causing a conformational change in the intracellular C-terminal GFP-tagged tail. The combination of the two antibodies had synergistic effects, increasing the level of cross-linking of de2−7-EGFR, but did not lead to enhanced cross-linking of EGFR. The results reveal new modes of receptor−antibody interactions for EGFR and de2−7-EGFR.

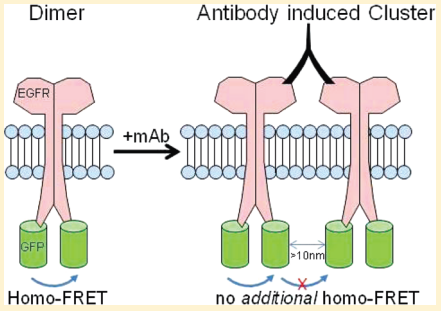

The epidermal growth factor receptor (EGFR) contributes to a number of processes that influence cancer development and progression, including cell proliferation, apoptosis, angiogenesis, and metastatic spread.[1,2] EGFR overexpression and mutation have been observed in a number of common cancers, including brain, lung, breast, colon, and prostate,[1] giving credence to the notion that a molecular understanding of EGFR activation will yield clinical benefits.[2,3] Signaling from the EGFR is generally initiated by binding of a ligand to the extracellular region, which leads to receptor tyrosine kinase dimerization or to conformational rearrangements within a preformed oligomeric complex.[4−7] However, some tumors express N-terminally truncated forms of the EGFR, such as the de2−7-EGFR, which are constitutively activated.

There is widespread interest in developing therapeutics that interfere with the inappropriate activation and signaling found in EGFR-dependent cancers.[3,8,9] EGFR antibodies offer a potentially powerful therapeutic agent against cancers driven by the EGFR pathway.[10−12] Indeed, several antibodies are already in the clinic and have been approved for the treatment of colorectal cancer (cetuximab and panitumumab) and head and neck cancer with external beam radiotherapy[13−16] or are in clinical development.[17]

EGFR antibodies are thought to function by blocking one or more of the steps that precede ligand-induced receptor activation: ligand binding, conformational transitions, and dimerization.[18,19] However, less appears to be known about how EGFR antibodies function on unliganded human EGFR receptor dimers because in solution extracellular domain fragments do not form dimers in the absence of ligand.[5] Indeed, there is a paucity of information about how the EGFR antibodies affect the oligomeric conformation of EGFR expressed in cells in the absence of ligand or other erbB receptors.

To address this issue, we have examined the effect of two EGFR antibodies (mAb528 and mAb806) on the aggregation state of wt-EGFR and the truncated mutant, de2−7-EGFR, on the surface of BaF/3 cells.[20,21]

Received: November 7, 2010
Revised: March 24, 2011
Published: April 15, 2011

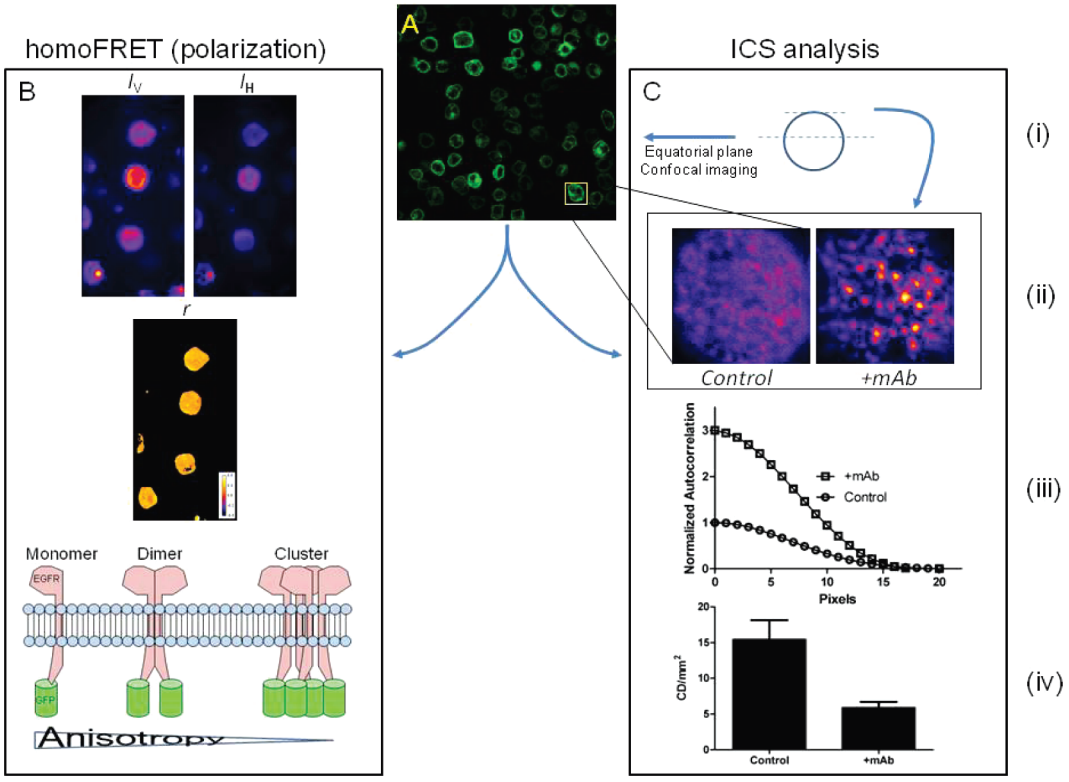

Figure 1. Homo-FRET and ICS data acquisition and analysis. (A) eGFP-tagged EGFR-expressing Baf/3 cells demonstrate a typical equatorial plane ring stain in a confocal image (60× water lens). The cells were subjected to the experimental protocol described (Experimental Procedures) and split in two. (B) For homo-FRET measurements, samples were imaged in wide field mode (100× oil lens) using polarized excitation and a dual viewer to record the vertical (I_V) and horizontal (I_H) images from which the steady-state anisotropy (r) image was calculated. Theory predicts a change in anisotropy values (r) depending on eGFP-tagged EGFR organization on the cell membrane (cartoon). Approximately 50 cells per sample were analyzed, for which averaged r values are listed in Table 1. (C) For ICS analysis, single cells were imaged in a confocal microscope (60× water lens, zoom 10). The focal plane was set to the top (or bottom) end of the cell to gain a view of the fluorescent signal at the membrane (i). Each image represents the accumulation of 50 scans in photon counting mode (ii). After image acquisition, 128 × 128 pixel regions of interest from single cells were selected and autocorrelated. Autocorrelation functions were fitted to a Gaussian-plus-offset function (iii), and the amplitude reciprocal value was calculated to estimate the cluster density (CD) of EGFR per square micrometer (iv). Approximately 10−20 cells were analyzed via ICS, and the values are plotted in Figure 3.

Table 1. Models of Antibody−Receptor Interactions and Qualitative Predictions of Image Correlation and Homotransfer and Anisotropy Experiments

no.	EGFR form interacting with mAb	receptor−antibody interaction[a]	comments	clustering (<200 nm)	homo FRET (<10 nm)
1	A, monomers	$Y + R \rightarrow RY$	binding	no change	none
2		$2R + Y \rightarrow RYR$	cross-linking	increase	no change or increase
3	B, dimers	$R_2 + Y \rightarrow RY + R$	dimer dissociation	decrease	decrease
4		$R_2 + Y \rightarrow R_2Y$	binding	no change	persistent, no change
5		$R_2 + Y \rightarrow R_2Y$	conformational change	no change	decrease or increase
6		$2R_2 + Y \rightarrow R_2YR_2$	dimer−dimer cross-linking	increase	persistent
7	C, oligomers	$R_n + nY \rightarrow R_nY_n$	binding	no change	persistent, no change
8		$R_n + nY \rightarrow R_nY^n$	conformational change	no change	increase or decrease
9		$2R_n + Y_n \rightarrow R_nY_nR_n$	cross-linking	increase	no change or increase
10		$R_{2n} + Y_n \rightarrow 2R_nY_n$	dissociation	decrease	decrease

[a] Y, antibody; R, EGFR.

Monoclonal antibody (mAb) 528 was produced by Kawamoto et al.[22] mAb528 is a murine equivalent of the C225 (cetuximab) antibody and displays very similar properties.[22] mAb528 binds to EGFR domain III and acts as a ligand antagonist, inhibiting the growth of EGFR-expressing cells both in vitro and in vivo.[22] mAb806 is a novel anti-EGFR-specific monoclonal antibody that was generated from mice immunized with de2−7-EGFR-transfected NR6 fibroblasts.[12,23] mAb806 targets not only the EGFR deletion variant, de2−7-EGFR, but also overexpressed wt-EGFR.[12,23−29] mAb806 binds poorly to normal tissue expressing physiological levels of the wtEGFR, including skin and liver, as demonstrated by extensive immunohistochemistry studies, and the first-in-man clinical trial of

the chimeric 806 antibody (ch806).[17,26] This specificity of mAb806 arises from its ability to recognize an epitope that is located in domain II of the extracellular region of EGFR, which is exposed only in cells containing overexpressed, truncated, or activated EGFR.[30−32]

To assess the effect of antibodies on the spatial organization of the EGFR and de2−7-EGFR, we used two techniques that are sensitive to aggregation on submicrometer and nanometer length scales, in a model cell system devoid of members of the endogenous erbB receptor family and ligands.[20,21] The experimental approaches are summarized in Figure 1. The combined information is used to distinguish between different antibody−receptor interactions (Table 1). Image correlation spectroscopy (ICS)[33−35] was used to characterize the change in the aggregation state of eGFP-tagged receptor clusters on a submicrometer scale.[21] ICS is a method developed to measure receptor cluster density and average size on cell surfaces.[34] It relies on the autocorrelation of fluorescence intensity fluctuations in space and is used to analyze confocal images of cells expressing fluorescently labeled receptors of interest.[34] Homo fluorescence resonance energy transfer (homo-FRET) was used to probe changes in conformation or oligomerization of the intracellular eGFP tags on a nanometer scale.[36,37] Homo-FRET involves the transfer of excited-state energy between fluorophores that are located within 1−10 nm of each other.[36,37] Because homo-FRET concerns the transfer of energy between identical fluorophores, it does not affect the emission spectrum or the fluorescence lifetime of the probes. However, homo-FRET is manifested as a decrease in the fluorescence anisotropy of the probes because emission can occur from acceptors that are in an orientation different from that of the initially photoexcited population.[38]

Analysis of antibody-induced changes on both the micro- and nanoscale provides valuable insights into the mechanism of action of these mAbs and improves our knowledge of EGFR functional biology.

EXPERIMENTAL PROCEDURES

Materials. Production and purification of mAb806 and mAb528 have been described previously.[29] Both antibodies were produced in the Biological Production Facility (Ludwig Institute for Cancer Research, Melbourne, Australia). The BaF/3 murine hemopoietic cell line expressing C-terminally tagged EGFR-eGFP constructs[21] or EGFR has also been described previously.[20,21]

de2−7-EGFR-eGFP Cloning. The extracellular domain of an untagged de2−7-EGFR construct, with exons 2−7 deleted, was excised from a pcDNA3 mammalian vector (Invitrogen) and used to replace the N-terminus of a wild-type EGFR construct within the C-terminally tagged eGFP vector, pEGFP.N3. The integrity of the recombined de2−7-EGFR-eGFP construct was confirmed by automated nucleotide sequencing.

Transfection of de2−7-EGFR-eGFP and Generation of Stable Cell Lines. de2−7-EGFR-eGFP cDNA was transfected into the BaF/3 murine hemopoietic cell line, as previously described.[20] The levels and stability of expression of de2−7-EGFR-eGFP in BaF/3 cells were assessed by FACS analysis on a FACStar (Becton and Dickinson, Franklin Lakes, NJ), using antibodies directed to the EGFR ectodomain (mAb 806, 20 μg/mL in PBS, 5% FCS, and 5 mM EDTA) and compared to expression levels of the established wt-EGFR-eGFP BaF/3 cell line.[21] Cells were maintained in culture under selection with 1.5 mg/mL G418 as previously described, with the exception that 1 μM AG1478 [kinase inhibitor, 4-(3-chloroanilino-6,7-dimethoxyquinazoline)mesylate[24]] was included in the medium to suppress the constitutive activation of the receptor during routine culturing. Prior to experimentation, cells were washed with PBS, resuspended in medium without AG1478, and further cultured for 3 days. The functional state and membrane expression of de2−7-EGFR-eGFP-expressing BaF/3 cells were further assessed by kinase assays, including the response to the EGFR inhibitor AG1478, via Western blot.[32]

Degree of EGFR-eGFP Aggregation Determined by Image Correlation Spectoscopy (ICS). ICS experiments were performed and analyzed as described previously.[21,39] Briefly, BaF/3 cells expressing either wt-EGFR-eGFP or de2−7-EGFR-eGFP were serum starved for 30 min and incubated for an additional 30 min with or without 50 μg/mL mAb528 or mAb806[29] at 4 °C prior to being fixed with a 4% PFA ice-cold solution. Half of the sample was taken for anisotropy measurements, and half was used for ICS analysis (see Figure 1 for details). Images representing the membrane-associated eGFP-tagged receptor were collected using a Bio-Rad MRC1000 scanning fluorescence confocal microscope [Nikon Plan Apo, 60× numerical aperture (NA) 1.2 water immersion lens, zoom 10, pinhole 2.4] with FITC emission optics (excitation at 488 nm and emission at 520 nm, with a 22 nm band-pass). Each image represents the accumulation of 50 scans in photon counting mode. ICS analysis was conducted on 128 × 128 pixel regions of interest (ROIs) representing areas of the cell surface. ROIs were autocorrelated using the Fourier Transform Math option in ImageJ (ImageJ, National Institutes of Health, Bethesda, MD), normalized by the number of pixels and average intensity squared, and corrected for background intensity. Data were fitted to a Gaussian-plus-offset function as described by Petersen et al.[34] The amplitude of the autocorrelation function [$g(0)$] and the full width at half-maximum (r) are related to the cluster density (CD, number of clusters per square micrometer) by the equation

$$\mathrm{CD} = [g(0)\pi r^2]^{-1} \quad (1)$$

A cluster can be a monomer, a dimer, or any arbitrarily sized oligomer. As a result, the cluster density does not provide information about the aggregation state of a molecule. However, changes in average aggregation state can be determined, provided the average number of molecules (N) per area remains constant.

Using the definition of the degree of aggregation (DA) of Petersen[34] as the average number of molecules per cluster (DA = N/CD), a change in the aggregation state can be represented by the ratio $DA_2/DA_1 = (CD_1/CD_2)(N_2/N_1)$. If identical cells are used (same expression level of molecules) and the molecules are retained at the cell surface during manipulations (this is why the antibody experiments were performed at 4 °C), then $N_2 = N_1$ and $DA_2/DA_1 = CD_1/CD_2$.

Steady-State Anisotropy Imaging. Imaging of steady-state anisotropy was conducted using an inverted microscope (TE2000U, Nikon, Inc.) supplemented with polarizing filters in the excitation path. Samples were excited using epi-illumination from a 470 nm light-emitting diode. The emitted fluorescence from labeled samples was collected using a 100× 1.25 NA oil objective (Nikon Plan-Fluor, Nikon, Inc.) through a filter set designed for FITC (Nikon FITC, DM505, EM 515−555 nm). Images of the parallel and perpendicular polarized emission were acquired simultaneously using a polarization splitter (Dual-Viewer, Optical Insights) imaged on an intensifier (Lambert Instruments) CCD camera (1300D Vosskuhler GmbH) combination.

The microscopy data were analyzed using a custom-written macro in ImageJ (data on LICR archive available upon request).

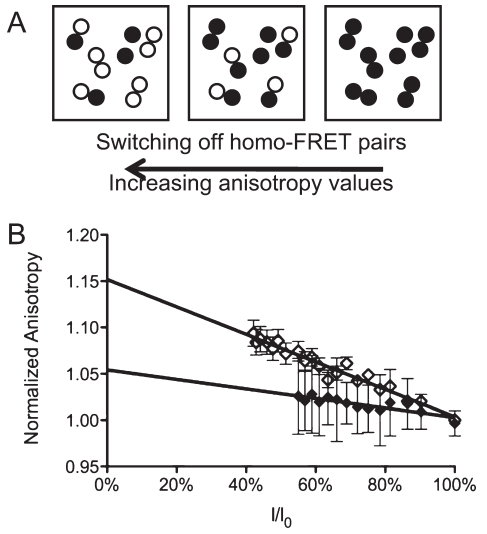

Figure 2. Photobleaching-induced changes in anisotropy reveal EGFR forms unliganded dimers and de2−7-EGFR forms dimers and oligomers. (A) Schematic representation of eGFP-tagged receptors on the cell membrane (●). Homo-FRET between two fluorophores in a dimer results in a decreased anisotropy compared to that of a singly labeled dimer due to energy transfer and light depolarization. Photobleaching of the sample (○) increases the proportion of eGFP-tagged dimers that contain only one fluorescent eGFP. This results in homo-FRET disruption and translates into increased anisotropy values. (B) Live Baf/3 cells expressing wt-EGFR-eGFP (empty symbols; $n = 15$) or de2−7-EGFR-eGFP (filled symbols; $n = 5$) were washed, immobilized on a coverslip, and imaged for ∼20 min while being constantly illuminated. Normalized anisotropy values are plotted as a function of the fractional intensity of the whole image (I/I_0, where I_0 is the intensity at t_0). The lines are linear fits to the data. Both the initial low r value [$r = 0.315 \pm 0.002$ and 0.325 ± 0.002 for wt- and de2−7-EGFR-eGFP, respectively (see Table 1)] and its increase upon sample bleaching imply homo-FRET between eGFP tags. The extrapolated anisotropy values when $I/I_0 = 0$ are 0.362 and 0.343 for wt- and de2−7-EGFR-eGFP, respectively. This result suggests that wt-EGFR-eGFP forms mainly unliganded dimers while de2−7-EGFR-eGFP forms a range of cluster sizes, including oligomers (see the text).

Images were corrected for camera offset (by capturing a dark image while the sample was not illuminated), nonuniform illumination (using an image of rhodamine 6G in solution), and buffer background (by subtracting the average background intensity calculated from a region in the image where no cells were visible). Each image, composed of both parallel (I_V) and perpendicular (I_H) emission components, was split in two and aligned. The steady-state anisotropy (r_i) in each pixel i was calculated according to

$$r_i = \frac{I_V - I_H}{I_V + 2GI_H} \tag{2}$$

where G is a correction factor taking into account the different transmission efficiencies of the parallel and perpendicular polarized emission components through the optical system (dichroic mirrors, filters, etc.) and was determined using an anisotropy standard [rhodamine 6G in water ($r = 0.012$)]. The calculated anisotropy values were corrected for the mixing of the polarization components caused by the high-numerical aperture objective as described by Axelrod.[40]

Single-cell anisotropies were computed from the anisotropy images using a mask generated in ImageJ by intensity thresholding. Image and anisotropy analysis programs were written as macros in the ImageJ platform, making analysis of many cells feasible (LICR archive). Generally, >50 cells were analyzed from each sample. The standard error of anisotropy values was ∼1% of the average r value.

Anisotropy Enhancement after Photobleaching. To determine the homotransfer between neighboring wt-EGFR-eGFP or de2−7-EGFR-eGFP molecules, we measured anisotropy during continuous photobleaching.[41] The measurements were taken on living cells without internalization inhibitors or fixatives. Cells were washed with 0.25% BSA in PBS buffer and immobilized on a coverslip using a 0.5% low-melting-point agarose gel. A sequence of fluorescence images (usually 40) containing both polarized components of the fluorescence (I_V and I_H) was acquired in parallel with the CCD camera under continuous illumination. Successive images exhibited decreased intensities with time due to photobleaching. The sequence of images was analyzed for anisotropy values (r), and a plot of r values versus the average image intensity remaining after photobleaching was generated. Any increase in r values with a decrease in intensity (increase in the extent of photobleaching) is an indication of the existence of homo-FRET between eGFP in the wt-EGFR-eGFP or de2−7 EGFR-eGFP complex (see Figure 2A for a schematic illustration).

Theory for the Interpretation of Anisotropy after Photobleaching. According to theory,[37] the anisotropy enhancement after photobleaching data can be interpreted in terms of oligomer size. For a monomeric population, the anisotropy is invariant to photobleaching:

$$r(f)^{\text{monomer}} = r_m \tag{3}$$

For a dimeric population, the predicted anisotropy, r, as a function of fluorophore labeling (f) is given by the equation

$$r^{\text{dimer}}(f) = (1-f)r_m + fr_d \tag{4}$$

where r_m is the anisotropy of a singly labeled dimer (partially photobleached, no homo-FRET) and r_d is the anisotropy of a doubly labeled dimer. For a tetrameric population

$$r^{\text{tetramer}}(f) = (1-f)^3 r_m + 3f(1-f)^2 r_d + 3f^2(1-f)r_{tri} + f^3 r_{tet} \tag{5}$$

In the context of a mixed monomer−dimer−tetramer population, the total anisotropy as a function of labeling is given by the equation

$$r^{\text{total}}(f) = ar(f)^{\text{monomer}} + br^{\text{dimer}}(f) + (1-a-b)r^{\text{tetramer}}(f) \tag{6}$$

where a is the monomer fraction, b is the dimer fraction, and $1 - a - b$ is the tetramer fraction. In principle, fitting anisotropy enhancement after photobleaching to the equation should yield the required fractions. However, this analysis requires bleaching to completion, which is undesirable in terms of cellular phototoxicity. Instead, as noted by Gangulay et al. (manuscript submitted for publication), the initial anisotropy and the linearly extrapolated anisotropy can be used.

When all molecules are labeled, i.e., $f = 1$

$$r^{\text{total}} = ar^{\text{monomer}} + br^{\text{dimer}} + (1-a-b)r^{\text{tetramer}} \tag{7}$$

The linearly extrapolated anisotropy, i.e., apparent $f = 0$, is obtained by extrapolating the tangent to the function near $f = 1$.

Table 2. Fluorescence Anisotropies of C-Terminally Tagged Receptor-eGFP Constructs in BaF/3 Cells

experiment	average anisotropy (r) (mean)	standard deviation	no. of measurements (N)	standard error
EGFR-eGFP	0.315	0.017	307	0.001
EGFR-eGFP with mAb528	0.313	0.015	111	0.001
de2−7-EGFR-eGFP	0.325	0.018	306	0.001
de2−7-EGFR-eGFP with mAb528	0.330	0.021	134	0.002
de2−7-EGFR-eGFP with mAb806	0.318	0.003	66	0.0004
EGFR-EGFR-eGFP heterodimer (no homo-FRET)	0.36−0.37[43]	not available	not available	not available
model protein-eGFP dimer (homo-FRET)	0.312[42]	not available	not available	not available

The functions describing monomer, dimer, and tetramer are

$$d[r(f)^{\text{monomer}}]/df = 0; \quad r(f = 0) = r_m \tag{8}$$

$$d[r(f)^{\text{dimer}}]/df = r_d - r_m; \quad r(f = 0) = r_m$$

$$d[r(f)^{\text{tetramer}}]/df = 3(r_{tet} - r_{tri}); \quad r(f = 0) = 3r_{tri} - 2r_{tet}$$

It is noted that the extrapolated anisotropies of monomers and dimers are equal to the monomeric anisotropy but the extrapolated anisotropy of tetramers (or other oligomers) is lower than the monomeric anisotropy, provided $r_m > r_{tri}$. This results from the fact that the anisotropy versus labeling curve for oligomers exhibits upward curvature. Using the linear extrapolations to $f = 0$

$$r^{\text{total}}(f \to 0) = (a + b)r_m + (1 - a - b)(3r_{tri} - 2r_{tet}) \tag{9}$$

It follows that the fraction of oligomeric (in this case tetrameric) forms can be determined from the extrapolated anisotropy after photobleaching (eq 9) and the other proportions obtained from the initial (unbleached anisotropy, eq 6). We note that this analysis is predicated on knowledge of the anisotropy values of the different oligomeric states but can provide a qualitative indication otherwise. For example, Bader[42] has estimated values for the relevant anisotropies for eGFP-tagged monomers, dimers, and oligomers: $r^{\text{monomer}} = 0.38$, $r^{\text{dimer}} = 0.31$, and $r^{\text{oligomer}} = 0.276$, respectively. In this case, eq 9 becomes

$$\begin{aligned} r^{\text{total}}(f \to 0) &= (a + b)r_m + (1 - a - b)(3r_{tri} - 2r_{tet}) \\ &= (a + b)r_m + (1 - a - b)(r^{\text{oligomer}}) \end{aligned} \tag{10}$$

Strategy for the Assignment of Antibody−Receptor Interactions. Table 1 provides a broad classification of antibody−receptor interactions together with qualitative, predicted outcomes of homo-FRET and ICS experiments. The interactions can be classified depending on the initial EGFR form, monomer, dimer, or higher-order oligomer (Table 1, column 1, A−C), and on whether they increase (dissociation; interactions 3 and 10), decrease (cross-linking; interactions 2, 6, and 9), or do not change (interactions 1, 4, 5, 7, and 8) the average number of aggregates per area (cluster density) on the cell surface. The availability of experimental homo-FRET and anisotropy data allows a further distinction between interactions that involve binding (interactions 1, 4, and 7) from those that involve conformational change (interactions 5 and 8).

Statistical Treatment of Data. To decide whether particular antibody treatments had significant effects on measured biophysical data, we applied a statistical significance test. Data were deemed significant if the population mean of the control data set was significantly different from the population mean of the antibody-treated data set. This was evaluated using the t test, from the population mean of the control (untreated), the population mean of the antibody-treated set, the standard deviation of the control, the standard deviation of the antibody-treated set, and the number of control and treatment samples. The risk threshold (p value) was set to 0.01 or 1%. Unless the mean, standard deviation, and sample number are specified, data are mentioned in the text as the mean ± 95% confidence limit, which was obtained from the sample mean and the sample standard error as means ± (1.96 × standard error).

RESULTS

In the Absence of Antibodies or Ligands on Living BaF/3 Cells, wt-EGFR-eGFP Forms Dimers and de2−7-EGFR-eGFP Forms Oligomers. Homo-FRET was used previously to determine the level of preformed wt-EGFR-eGFP dimers on the surface of cells.[42,43] To compare the oligomeric state of wt-EGFR-eGFP and de2−7-EGFR-eGFP in the absence of antibodies, ligands, or other erbB receptors on the surface of living BaF/3 cells, we measured homo-FRET using the steady-state fluorescence anisotropy of the eGFP tag. The steady-state anisotropies of the fluorescently tagged receptors are listed in Table 2. The anisotropies of the membrane receptors wt-EGFR-eGFP (0.315 ± 0.002) and de2−7-EGFR-eGFP (0.325 ± 0.002) in BaF/3 cells were reduced compared to the anisotropy of rotationally immobile, monomeric eGFP (0.38[42]) or of EGFR-EGFR-eGFP heterodimers (0.36[43]) but closer to the values reported for dimeric eGFP-tagged molecules undergoing homo-FRET (0.312[42]). To confirm that the low anisotropy was indeed due to homotransfer, gradual photobleaching experiments were performed. When the whole cells are progressively photobleached, the probability of homotransfer will be reduced, because oligomers containing one fluorescent eGFP and the rest photobleached cannot participate in homotransfer (Figure 2A). The results of the photobleaching experiments for both wt-EGFR-eGFP- and de2−7-EGFR-eGFP-expressing BaF/3 cells are shown in Figure 2B. The data demonstrate an increase in the anisotropy of emission (normalized r) with decreasing intensity (increasing degree of photobleaching, I/I_0). This indicates the presence of homotransfer between (at least) two eGFP moieties within an EGFR-eGFP oligomer. From a linear fit of the wt-EGFR-eGFP data, the extrapolated value of the anisotropy for 100% photobleaching was 0.36. This value represents the anisotropy of eGFP in the absence of homotransfer. This value is close to the reported anisotropy of immobile eGFP[42,43] and suggests that the eGFP moieties within the wt-EGFR-eGFP dimers are motionally restricted. Bader has demonstrated that for eGFP-tagged proteins the fraction of dimerization can be

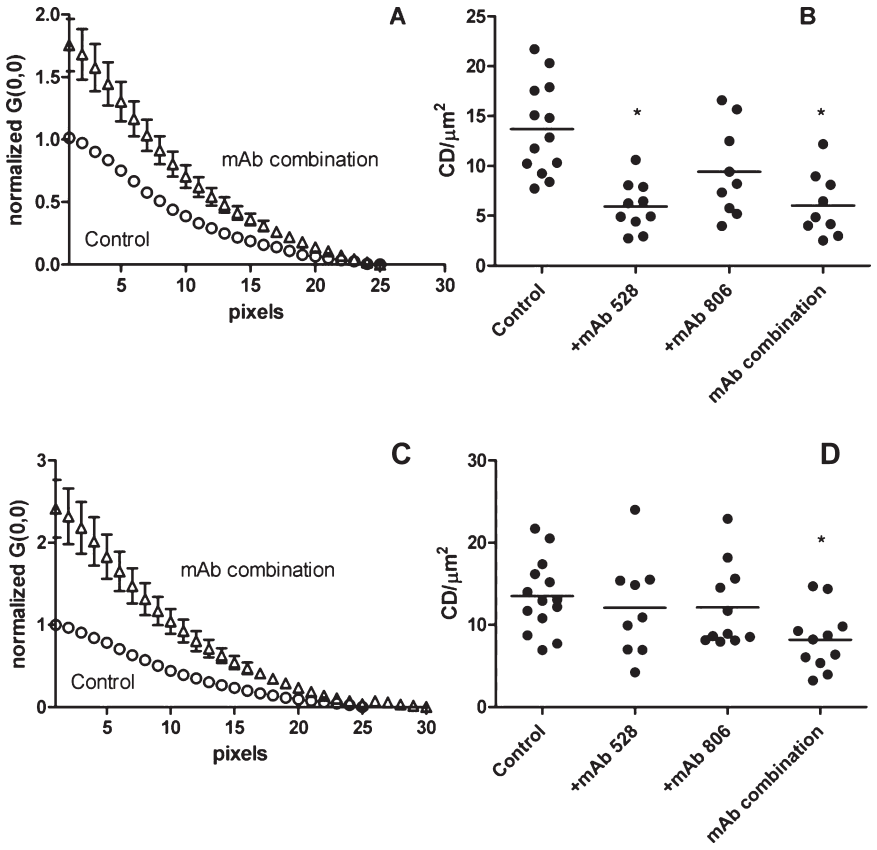

Figure 3. Antibody- and receptor-dependent antibody-induced receptor cross-linking. Normalized autocorrelation functions [$G(0,0)$] representing ICS experiments (A and C). Baf/3 cells expressing wt-EGFR-eGFP (A) or de2−7-EGFR-eGFP (C) were washed with PBS and serum starved for 30 min followed by a 30 min incubation at 4 °C in the absence (Control) or presence of 50 μg/mL (total protein) single mAb or a combination as indicated. Data are averages ± the standard error from 9 to 14 cells/treatment. For the sake of clarity, only results from the control and a representing mAb experiment are shown. (B and D) Cluster density (CD, the number of clusters per square micrometer) of wt-EGFR-eGFP (B) or de2−7-EGFR-eGFP (D) as a function of antibody used. Each point represents data from a single cell. Asterisks signify Student's t test significance ($p < 0.01$). A decrease in the density of clusters compared to control indicates an increase in the level of the aggregation state (at a constant receptor number).

estimated from anisotropy measurements.[42] Using the reported anisotropy value of 0.381 (or extrapolated anisotropy of 0.36) corresponding to monomeric EGFR-eGFP and the anisotropy value of 0.312 corresponding to dimeric EGFR-eGFP, we estimate a fractional fluorescence of dimerization of 95% (93% using 0.36 as the monomeric anisotropy) in the BaF/3 cells (eq 7, for which $a + b = 1$). These results are in accordance with previous conclusions from our laboratory based on image correlation spectroscopy experiments that wt-EGFR-eGFP is predominantly dimeric in the absence of a ligand on BaF/3 cells.[21] de2−7-EGFR-eGFP also demonstrated depolarized emission, with an average steady-state anisotropy of 0.325. Making the same calculation as for EGFR-eGFP, we compute 80% dimers for de2−7-EGFR-eGFP. However, the photobleaching anisotropy data revealed behavior different from that of the wild-type receptor. Bleaching experiments with de2−7-EGFR-eGFP also showed anisotropy enhancement, but the extrapolated value of the anisotropy for 100% photobleaching was, on average, significantly lower (r = 0.34), i.e., as an indication of the presence of higher-order oligomers in the de2−7-EGFR-eGFP population. Because the de2−7-EGFR-eGFP bleaching experiment showed population variation (see error bars), a precise figure for the proportions of dimeric and oligomeric de2−7-EGFR-eGFP forms could not be derived. Given the initial anisotropy of 0.325, and an extrapolated bleach anisotropy ranging from 0.325 to 0.38, the proportion of dimers varies from 0 to 80%, the proportion of oligomers varies from 0 to 53%, and the proportion of monomers varies from 20 to 47% (eqs 7 and 10). The average values correspond to a de2−7-EGFR-eGFP population distribution consisting of 40% monomer, 20% dimer, and 40% oligomer. We conclude that while wt-EGFR-eGFP is predominantly dimeric, de2−7-EGFR-eGFP is clustered to varying extents with a substantial proportion in dimer and oligomer forms. These conclusions apply to our BaF/3 cell system under our measurement conditions (no ligand, no endogenous receptors, and live cells) with receptors expressed at normal levels (i.e., 50−70000 receptors/cell).

Effect of EGFR Antibodies on wt-EGFR-eGFP Clustering in BaF/3 Cells. To assess whether EGFR antibodies disperse, aggregate, or alter the cell surface distribution of the EGFR dimers and oligomers, we used ICS to determine the average density of the EGFR clusters and any changes caused by antibody binding. The ICS results, summarized in Figure 3, show that addition of antibody mAb528 decreased the density of wt-EGFR-eGFP aggregates on the cell surface (Figure 3A,B). Because these experiments were conducted under conditions where EGFR is retained on the cell surface at a constant number (at 4 °C), the decrease in aggregate density implies an increase in the association state by a factor of 2.3-fold per EGFR cluster. The difference in the cluster densities of the control (mean = 13.7; SD = 4.6;

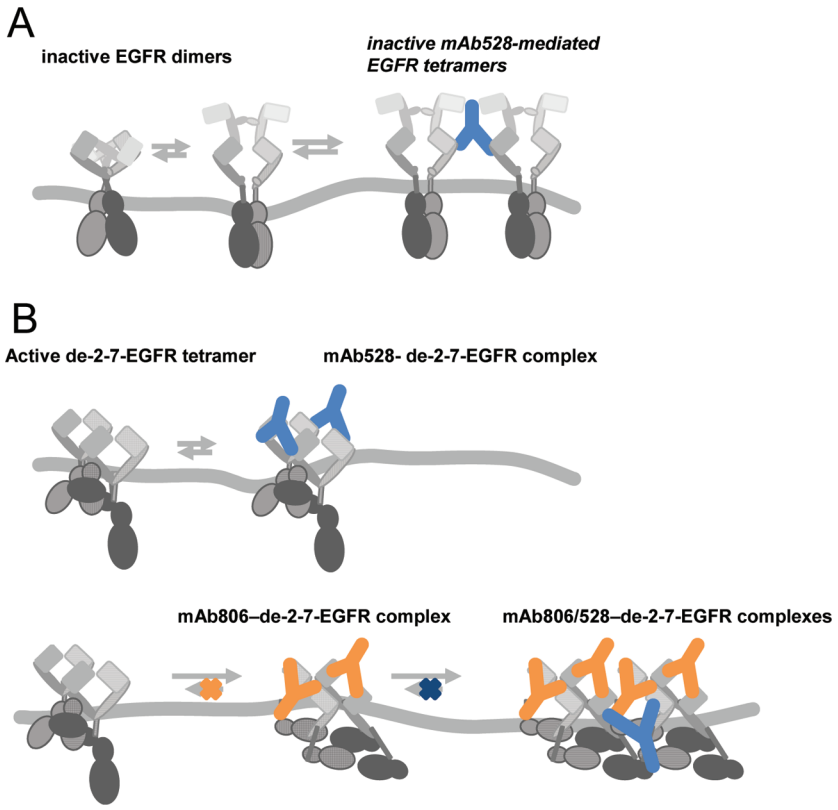

Figure 4. Model of antibody−receptor interactions for EGFR and de2−7-EGFR. (A) Unliganded, dimerized wt-EGFR-eGFP (identified using homo-FRET). mAb528 can from a head-to-head cross-link between two dimers forming an inactive tetramer. We propose that the spacing between the antibody Fab arms prevents asymmetric kinase−kinase interactions between dimers in the antibody-mediated tetrameric complex (see phosphorylation Western blots in Figure S1 of the Supporting Information). (B) de2−7 EGFR-eGFP forms constitutively active oligomers (tetramers). mAb528 binds but does not alter the cluster size or conformation of de2−7-EGFR. mAb806 causes a conformational change that rearranges the C-terminal domains, altering access to intracellular effectors. Because de2−7-EGFR forms constitutively active dimers and oligomers (see phosphorylation Western blots in Figure S2 of the Supporting Information), single mAb treatments did not cluster it further. However, the combination of both antibodies may facilitate a conformational change that results in cross-linking.

$N = 13$) and mAb528-treated samples (mean = 5.9; SD = 2.5; $N = 10$) is statistically significant ($p = 0.01\%$). Taken together with the homo-FRET results, these results suggest that mAb528 causes clustering of a proportion of the wt-EGFR-eGFP into higher-order aggregates. Addition of mAb806 did not significantly affect the density of aggregates (Figure 3B; mean = 9.4; SD = 4.6; $N = 9$; $p = 4.4\%$), probably because mAb806 binds only a minor subset, if at all, of the wt-EGFR on the BaF/3 cell surface.[17,26] As expected, the combination of mAb528 and mAb806 did significantly increase the level of clustering of wt-EGFR-eGFP (Figure 3b; mean = 6.0; SD = 3.2; $N = 9$; $p = 0.3\%$) but not significantly beyond that observed with Ab528 alone ($p = 94\%$, comparing mAb528 treatment with combination treatment).

Effect of EGFR Antibodies on de2−7-EGFR-eGFP Clustering in BaF/3 Cells. The results for similar ICS experiments with de2−7-EGFR-eGFP on BaF/3 cells are shown in panels C and D of Figure 3. Neither mAb528 (mean = 12.1; SD = 6.1; $N = 9$; $p = 18.3\%$) nor mAb806 in complex with de2−7-EGFR-eGFP (mean = 12.5; SD = 5.2; $N = 20$; $p = 13.0\%$) altered significantly the average cluster density of de2−7-EGFR-eGFP (mean = 15.5; SD = 6.7; $N = 26$). However, in the presence of both mAbs, there was a significant change in the cell surface distribution of de2−7-EGFR-eGFP (mean = 8.2; SD = 3.8; $N = 11$; $p = 0.2\%$). The cluster density decreased by 2.2-fold; i.e., there was an increase in the average level of the association state of a factor of∼2.

Effect of EGFR Antibodies on the Fluorescence Anisotropy of the C-Terminal eGFP Tags. In general, changes in emission anisotropy can be attributed to (1) changes in the motion of the eGFP probe or (2) changes in the homotransfer between probes or a combination of both. The extrapolated anisotropy (0.36) from the photobleaching experiments indicates that the eGFP moiety is close to immobile within the wt-EGFR-eGFP dimers during the excited-state lifetime of the eGFP probe. Therefore, the steady-state anisotropy provides a measure of changes in homo-FRET that might accompany antibody binding, changes in the extent of oligomerization, or changes in the distance and orientation between the C-terminal eGFP tags. Measurements taken on several sets of cells ($n > 50$ cells per measurement) showed negligible changes in anisotropy when mAb528 is bound to the wt-EGFR-eGFP [wt-EGFR-eGFP (mean = 0.315; SD = 0.017; $N = 307$) and the mAb528−wt-EGFR-eGFP complex (mean = 0.313; SD = 0.015; $N = 111$), $p = 27\%$ (Table 2)]. The sustained low levels of anisotropy (<0.36) indicate the persistence of homo-FRET between eGFP moieties within the receptor dimer population but no measurable change even under conditions where the average aggregate size increases by a factor of 2. In contrast, while binding of mAb528 to de2−7-EGFR-eGFP produced no significant changes in anisotropy [$p = 1.1\%$ (data in Table 2)], the binding of mAb806 decreased the anisotropy of de2−7-EGFR-eGFP by a small but statistically significant amount [$p = 0.2\%$ (Table 2)]. Because no change in

dx.doi.org/10.1021/bi101785h |*Biochemistry* 2011, 50, 3581–3590

cluster density of de2−7-EGFR-eGFP was observed, we conclude mAb806 produces a conformational change in the preformed de2−7-EGFR-eGFP oligomers.

DISCUSSION

Our studies were designed to examine the effect of anti-EGFR antibodies on the association and conformational states of unliganded EGFR and de2−7-EGFR oligomers on the surface of cells. It is important to stress that the model cellular system (BaF/3 cells) was chosen because there is no interference from members of the endogenous EGFR family or ligands.[20] This allows the antibody-mediated effects to be unequivocally assigned to antibody−receptor interactions without the potential for hetero-oligomerization (with erbB2, erbB3, erbB4, or other receptors) or ligand-induced oligomerization that could otherwise confound interpretation of experiments of this type. We stress that our experimental approaches and systems represent a model system for evaluating the relative effects of antibody treatments on the biophysical states of receptors. The receptor/cell systems employed, together with the microscopy analyses, allow examination of the effects of antibodies on both the nanometer (1−10 nm) and submicrometer (250 nm) scales.

We have identified several new antibody−receptor interactions for these classes of antibodies that are relevant to oligomeric receptors. Figure 4 summarizes the novel antibody−receptor interactions identified for EGFR and de2−7-EGFR from this study. The mAb528−EGFR interaction is shown in Figure 4A. In addition to the role of mAb528 in blocking ligand binding and preventing the tether−untether transition in the monomeric state, it can trap unliganded inactive dimers into inactive, higher-order oligomers and prevent the required kinase−kinase interaction(s) needed to activate the kinase domain. A recent study biochemically isolated antibody-mediated weakly active tetramers of erbB2/erbB1 receptors,[44] and earlier work identified cross-linking of unliganded monomeric EGFR receptors into dimers.[45,46] To the best of our knowledge, this is the first report of an antibody-mediated inactive dimer to inactive tetramer transition on the surface of cells. This transition is distinct from the EGF-mediated dimer to tetramer transition that occurs during EGFR activation in BaF/3 cells[21] and suggests that the antibody-mediated tetramer has a structure different from the EGF-mediated one. Our phosphorylation blots confirm that mAb528 does not activate the receptor, but as expected, EGF stimulates the kinase activity (see the Supporting Information).

The interaction of de2−7-EGFR and mAb806 is shown in Figure 4B. A conformational change within the de2−7-EGFR oligomeric receptors, induced by mAb806 binding, has been identified from the combined clustering and homo-FRET measurements (Figure 4B). mAb806 is thought to trap a transitional form of the EGFR ectodomain that is populated during receptor activation.[31,32] Our data reveal that mAb806 can also cause a conformational rearrangement within de2−7-EGFR oligomers that it is propagated to the C-terminus. mAb806 does not inactivate the receptor kinase of de2−7-EGFR [as shown by phosphorylation blots (see the Supporting Information)], but it has been shown to effect levels of site-specific phosphorylation in cultured cells.[47]

The combination treatment with the antibodies reveals synergistic effects on cross-linking. Neither mAb528 (Figure 4B) nor mAb806 by itself enhances cross-linking of de2−7-EGFR; however, the presence of both antibodies increases the level of receptor cross-linking. We propose that mAb806 causes a conformational change that allows interoligomer cross-links to be formed by mAb528 (Figure 4B). Interestingly, combination treatments appear to be more effective in inhibiting tumor growth in mouse xenographs than application of each antibody alone.[29] Although comparison of different experiments on different systems should be treated with caution, it is tempting to speculate that the synergistic antibody effect on tumor xenograph growth might be related to the synergistic antibody effect on cross-linking of de2−7-EGFR as revealed for the first time in this study.

It is noteworthy that various studies have identified that bivalent IgG (mAb EGFR antibodies), as opposed to monovalent Fc or Fab fragments (from mAb EGFR antibodies), has enhanced antiproliferative effects on cells. The requirement for bivalency mechanistically links the antibody-induced receptor cross-linking observed in this study to the overall inhibitory effect of antibodies.[45,46,48] The ability to form inactive tetramers or receptor lattices by combination antibodies has also been proposed as a mechanism for downregulating erbB2.[18,44]

In a recent review,[19] Ferguson emphasized the importance of antibodies in halting one or more of the steps involved in the ligand-induced monomer to dimer transition leading to activation of the kinase. In the context of the available structures of antibody−receptor fragments, Ferguson suggests that these antibodies work by either blocking ligand binding, stopping the transition between the tethered monomer and the untethered dimer, or blocking one or more interfaces that are involved in receptor dimerization. These studies are relevant to our understanding of the way antibodies might work on a monomeric population of receptors, i.e., by preventing any further oligomerization required to activate the receptor. However, receptor tyrosine kinases can also exist in other oligomeric forms.[49] Our study complements and extends these findings into the cellular environment where unliganded dimeric and/or oligomeric receptors are present.[21,39,50,51] Subcellular microdomains on the cell surface can also provide regions of high local concentration where dimerization and oligomerization are enhanced. The importance of understanding antibody-mediated effects on oligomeric, as distinct from monomeric, receptors assumes relevance when it is recognized that EGFR forms dimers and, in the case of de2−7-EGFR, dimers and oligomers, and the significance of these dimeric and oligomeric forms increases in cancer cells due to a combination of factors, including overexpression,[51] mutation (as revealed for de2−7-EGFR in this study), and/or altered lipid environments.[52]

The results presented here suggest that the interaction of antibodies with cell surface receptors requires consideration of multiple oligomeric states. Use of biophysical tools to elucidate these states might help in the future design of therapeutics with improved properties.

ASSOCIATED CONTENT

Supporting Information. Experimental methods for EGFR phosphorylation Western blots. This material is available free of charge via the Internet at http://pubs.acs.org.

AUTHOR INFORMATION

Corresponding Author

*A.H.A.C.: Cell Biophysics Laboratory, Swinburne University of Technology, Centre for Microphotonics, P.O. Box 218, Hawthorn, Victoria 3122, Australia; telephone, +61-3-9214-5719; fax, +61-3-9214-5435; e-mail, aclayton@swin.edu.au. A.M.S.: Ludwig Institute for Cancer Research, Melbourne-Austin Branch, Austin Hospital, Studley Road, Heidelberg, Victoria

3084, Australia; telephone, +61-3-9496-5726; fax, +61-3-9496-5334; e-mail, andrew.scott@ludwig.edu.au.

Funding Sources

A.H.A.C. was partially supported by an R. D. Wright Biomedical Career Development Award from the Australian National Health and Medical Research Council (NHMRC). This work was also supported by NHMRC Grants 280918 and 433624 and NHMRC Program 280912.

■ ABBREVIATIONS

EGFR, epidermal growth factor receptor; wt, wild type; de2−7, truncated EGFR mutant; mAb, monoclonal antibody; ICS, image correlation spectroscopy; eGFP, enhanced green fluorescent protein; SD, standard deviation.

■ REFERENCES

(1) Burgess, A. W. (2008)EGFR family: Structure physiology signalling and therapeutic targets. *Growth Factors 26*, 263–274.

(2) Mendelsohn, J., and Baselga, J. (2006)Epidermal growth factor receptor targeting in cancer. *Semin. Oncol. 33*, 369–385.

(3) Mendelsohn, J., and Baselga, J. (2003)Status of epidermal growth factor receptor antagonists in the biology and treatment of cancer. *J. Clin. Oncol. 21*, 2787–2799.

(4) Jiang, G., and Hunter, T. (1999)Receptor signaling: When dimerization is not enough. *Curr. Biol. 9*, R568–R571.

(5) Lemmon, M. A., Bu, Z., Ladbury, J. E., Zhou, M., Pinchasi, D., Lax, I., Engelman, D. M., and Schlessinger, J. (1997)Two EGF molecules contribute additively to stabilization of the EGFR dimer. *EMBO J. 16*, 281–294.

(6) Schlessinger, J. (2000)Cell signaling by receptor tyrosine kinases. *Cell 103*, 211–225.

(7) Yarden, Y., and Sliwkowski, M. X. (2001)Untangling the ErbB signalling network. *Nat. Rev. 2*, 127–137.

(8) Arteaga, C. (2003)Targeting HER1/EGFR: A molecular approach to cancer therapy. *Semin. Oncol. 30*, 3–14.

(9) Mendelsohn, J. (2000)Blockade of receptors for growth factors: An anticancer therapy—the fourth annual Joseph H. Burchenal American Association of Cancer Research Clinical Research Award Lecture. *Clin. Cancer Res. 6*, 747–753.

(10) Herbst, R. S., and Shin, D. M. (2002)Monoclonal antibodies to target epidermal growth factor receptor-positive tumors: A new paradigm for cancer therapy. *Cancer 94*, 1593–1611.

(11) Snyder, L. C., Astsaturov, I., and Weiner, L. M. (2005)Overview of monoclonal antibodies and small molecules targeting the epidermal growth factor receptor pathway in colorectal cancer. *Clin. Colorectal Cancer 5* (Suppl. 2), S71–S80.

(12) Johns, T. G., Stockert, E., Ritter, G., Jungbluth, A. A., Huang, H. J., Cavenee, W. K., Smyth, F. E., Hall, C. M., Watson, N., Nice, E. C., Gullick, W. J., Old, L. J., Burgess, A. W., and Scott, A. M. (2002)Novel monoclonal antibody specific for the de2−7 epidermal growth factor receptor (EGFR) that also recognizes the EGFR expressed in cells containing amplification of the EGFR gene. *Int. J. Cancer 98*, 398–408.

(13) Bernier, J., and Schneider, D. (2007)Cetuximab combined with radiotherapy: An alternative to chemoradiotherapy for patients with locally advanced squamous cell carcinomas of the head and neck? *Eur. J. Cancer 43*, 35–45.

(14) Galizia, G., Lieto, E., De Vita, F., Orditura, M., Castellano, P., Troiani, T., Imperatore, V., and Ciardiello, F. (2007)Cetuximab, a chimeric human mouse anti-epidermal growth factor receptor monoclonal antibody, in the treatment of human colorectal cancer. *Oncogene 26*, 3654–3660.

(15) Saltz, L., Easley, C., and Kirkpatrick, P. (2006)Panitumumab. *Nat. Rev. Drug Discovery 5*, 987–988.

(16) Zhang, W., Gordon, M., and Lenz, H. J. (2006)Novel approaches to treatment of advanced colorectal cancer with anti-EGFR monoclonal antibodies. *Ann. Med. 38*, 545–551.

(17) Scott, A. M., Lee, F. T., Tebbutt, N., Herbertson, R., Gill, S. S., Liu, Z., Skrinos, E., Murone, C., Saunder, T. H., Chappell, B., Papenfuss, A. T., Poon, A. M., Hopkins, W., Smyth, F. E., MacGregor, D., Cher, L. M., Jungbluth, A. A., Ritter, G., Brechbiel, M. W., Murphy, R., Burgess, A. W., Hoffman, E. W., Johns, T. G., and Old, L. J. (2007)A phase I clinical trial with monoclonal antibody ch806 targeting transitional state and mutant epidermal growth factor receptors. *Proc. Natl. Acad. Sci. U.S.A. 104*, 4071–4076.

(18) Friedman, L. M., Rinon, A., Schechter, B., Lyass, L., Lavi, S., Bacus, S. S., Sela, M., and Yarden, Y. (2005)Synergistic down-regulation of receptor tyrosine kinases by combinations of mAbs: Implications for cancer immunotherapy. *Proc. Natl. Acad. Sci. U.S.A. 102*, 1915–1920.

(19) Schmitz, K. R., and Ferguson, K. M. (2009)Interaction of antibodies with ErbB receptor extracellular regions. *Exp. Cell Res. 315*, 659–670.

(20) Walker, F., Hibbs, M. L., Zhang, H. H., Gonez, L. J., and Burgess, A. W. (1998)Biochemical characterization of mutant EGF receptors expressed in the hemopoietic cell line BaF/3. *Growth Factors 16*, 53–67.

(21) Clayton, A. H., Walker, F., Orchard, S. G., Henderson, C., Fuchs, D., Rothacker, J., Nice, E. C., and Burgess, A. W. (2005)Ligand-induced dimer-tetramer transition during the activation of the cell surface epidermal growth factor receptor-A multidimensional microscopy analysis. *J. Biol. Chem. 280*, 30392–30399.

(22) Kawamoto, T., Sato, J. D., Le, A., Polikoff, J., Sato, G. H., and Mendelsohn, J. (1983)Growth stimulation of A431 cells by epidermal growth factor: Identification of high-affinity receptors for epidermal growth factor by an anti-receptor monoclonal antibody. *Proc. Natl. Acad. Sci. U.S.A. 80*, 1337–1341.

(23) Mishima, K., Johns, T. G., Luwor, R. B., Scott, A. M., Stockert, E., Jungbluth, A. A., Ji, X. D., Suvarna, P., Voland, J. R., Old, L. J., Huang, H. J., and Cavenee, W. K. (2001)Growth suppression of intracranial xenografted glioblastomas overexpressing mutant epidermal growth factor receptors by systemic administration of monoclonal antibody (mAb) 806, a novel monoclonal antibody directed to the receptor. *Cancer Res. 61*, 5349–5354.

(24) Johns, T. G., Luwor, R. B., Murone, C., Walker, F., Weinstock, J., Vitali, A. A., Perera, R. M., Jungbluth, A. A., Stockert, E., Old, L. J., Nice, E. C., Burgess, A. W., and Scott, A. M. (2003)Antitumor efficacy of cytotoxic drugs and the monoclonal antibody 806 is enhanced by the EGF receptor inhibitor AG1478. *Proc. Natl. Acad. Sci. U.S.A. 100*, 15871–15876.

(25) Johns, T. G., Mellman, I., Cartwright, G. A., Ritter, G., Old, L. J., Burgess, A. W., and Scott, A. M. (2005)The antitumor monoclonal antibody 806 recognizes a high-mannose form of the EGF receptor that reaches the cell surface when cells over-express the receptor. *FASEB J. 19*, 780–782.

(26) Jungbluth, A. A., Stockert, E., Huang, H. J., Collins, V. P., Coplan, K., Iversen, K., Kolb, D., Johns, T. J., Scott, A. M., Gullick, W. J., Ritter, G., Cohen, L., Scanlan, M. J., Cavenee, W. K., and Old, L. J. (2003)A monoclonal antibody recognizing human cancers with amplification/overexpression of the human epidermal growth factor receptor. *Proc. Natl. Acad. Sci. U.S.A. 100*, 639–644.

(27) Luwor, R. B., Johns, T. G., Murone, C., Huang, H. J., Cavenee, W. K., Ritter, G., Old, L. J., Burgess, A. W., and Scott, A. M. (2001) Monoclonal antibody 806 inhibits the growth of tumor xenografts expressing either the de2−7 or amplified epidermal growth factor receptor (EGFR) but not wild-type EGFR. *Cancer Res. 61*, 5355–5361.

(28) Luwor, R. B., Zhu, H. J., Walker, F., Vitali, A. A., Perera, R. M., Burgess, A. W., Scott, A. M., and Johns, T. G. (2004)The tumor-specific de2−7 epidermal growth factor receptor (EGFR) promotes cells survival and heterodimerizes with the wild-type EGFR. *Oncogene 23*, 6095–6104.

(29) Perera, R. M., Narita, Y., Furnari, F. B., Gan, H. K., Murone, C., Ahlkvist, M., Luwor, R. B., Burgess, A. W., Stockert, E., Jungbluth, A. A., Old, L. J., Cavenee, W. K., Scott, A. M., and Johns, T. G. (2005)

Treatment of human tumor xenografts with monoclonal antibody 806 in combination with a prototypical epidermal growth factor receptor-specific antibody generates enhanced antitumor activity. *Clin. Cancer Res. 11*, 6390–6399.

(30) Chao, G., Cochran, J. R., and Wittrup, K. D. (2004)Fine epitope mapping of anti-epidermal growth factor receptor antibodies through random mutagenesis and yeast surface display. *J. Mol. Biol. 342*, 539–550.

(31) Johns, T. G., Adams, T. E., Cochran, J. R., Hall, N. E., Hoyne, P. A., Olsen, M. J., Kim, Y. S., Rothacker, J., Nice, E. C., Walker, F., Ritter, G., Jungbluth, A. A., Old, L. J., Ward, C. W., Burgess, A. W., Wittrup, K. D., and Scott, A. M. (2004)Identification of the epitope for the epidermal growth factor receptor-specific monoclonal antibody 806 reveals that it preferentially recognizes an untethered form of the receptor. *J. Biol. Chem. 279*, 30375–30384.

(32) Walker, F., Orchard, S. G., Jorissen, R. N., Hall, N. E., Zhang, H. H., Hoyne, P. A., Adams, T. E., Johns, T. G., Ward, C., Garrett, T. P., Zhu, H. J., Nerrie, M., Scott, A. M., Nice, E. C., and Burgess, A. W. (2004)CR1/CR2 interactions modulate the functions of the cell surface epidermal growth factor receptor. *J. Biol. Chem. 279*, 22387–22398.

(33) Kolin, D. L., and Wiseman, P. W. (2007)Advances in image correlation spectroscopy: Measuring number densities, aggregation states, and dynamics of fluorescently labeled macromolecules in cells. *Cell Biochem. Biophys. 49*, 141–164.

(34) Petersen, N. O., Brown, C., Kaminski, A., Rocheleau, J., Srivastava, M., and Wiseman, P. W. (1998)Analysis of membrane protein cluster densities and sizes in situ by image correlation spectroscopy. *Faraday Discuss.* 289–305.

(35) Wiseman, P. W., Hoddelius, P., Petersen, N. O., and Magnusson, K. E. (1997)Aggregation of PDGF-β receptors in human skin fibroblasts: Characterization by image correlation spectroscopy (ICS). *FEBS Lett. 401*, 43–48.

(36) Tramier, M., and Coppey-Moisan, M. (2008)Fluorescence anisotropy imaging microscopy for homo-FRET in living cells. *Methods Cell Biol. 85*, 395–414.

(37) Yeow, E. K., and Clayton, A. H. (2007)Enumeration of oligomerization states of membrane proteins in living cells by homo-FRET spectroscopy and microscopy: Theory and application. *Biophys. J. 92*, 3098–3104.

(38) Lakowicz, J. R. (1999) *Principles of fluorescence spectroscopy*, 2nd ed., Kluwer Academic/Plenum Publishers, New York.

(39) Clayton, A. H., Tavarnesi, M. L., and Johns, T. G. (2007) Unligated epidermal growth factor receptor forms higher order oligomers within microclusters on A431 cells that are sensitive to tyrosine kinase inhibitor binding. *Biochemistry 46*, 4589–4597.

(40) Axelrod, D. (1989)Fluorescence polarization microscopy. *Methods Cell Biol. 30*, 333–352.

(41) Varma, R., and Mayor, S. (1998)GPI-anchored proteins are organized in submicron domains at the cell surface. *Nature 394*, 798–801.

(42) Bader, A. N., Hofman, E. G., Voortman, J., en Henegouwen, P. M., and Gerritsen, H. C. (2009)Homo-FRET imaging enables quantification of protein cluster sizes with subcellular resolution. *Biophys. J. 97*, 2613–2622.

(43) Lidke, D. S., Nagy, P., Barisas, B. G., Heintzmann, R., Post, J. N., Lidke, K. A., Clayton, A. H., Arndt-Jovin, D. J., and Jovin, T. M. (2003) Imaging molecular interactions in cells by dynamic and static fluorescence anisotropy (rFLIM and emFRET). *Biochem. Soc. Trans. 31*, 1020–1027.

(44) Furuuchi, K., Berezov, A., Kumagai, T., and Greene, M. I. (2007)Targeted antireceptor therapy with monoclonal antibodies leads to the formation of inactivated tetrameric forms of ErbB receptors. *J. Immunol. 178*, 1021–1029.

(45) Fan, Z., Lu, Y., Wu, X., and Mendelsohn, J. (1994)Antibody-induced epidermal growth factor receptor dimerization mediates inhibition of autocrine proliferation of A431 squamous carcinoma cells. *J. Biol. Chem. 269*, 27595–27602.

(46) Fan, Z., Masui, H., Altas, I., and Mendelsohn, J. (1993)Blockade of epidermal growth factor receptor function by bivalent and monovalent fragments of 225 anti-epidermal growth factor receptor monoclonal antibodies. *Cancer Res. 53*, 4322–4328.

(47) Johns, T. G., Perera, R. M., Vernes, S. C., Vitali, A. A., Cao, D. X., Cavenee, W. K., Scott, A. M., and Furnari, F. B. (2007)The efficacy of epidermal growth factor receptor-specific antibodies against glioma xenografts is influenced by receptor levels, activation status, and heterodimerization. *Clin. Cancer Res. 13*, 1911–1925.

(48) Perez-Torres, M., Guix, M., Gonzalez, A., and Arteaga, C. L. (2006)Epidermal growth factor receptor (EGFR) antibody down-regulates mutant receptors and inhibits tumors expressing EGFR mutations. *J. Biol. Chem. 281*, 40183–40192.

(49) Lemmon, M. A., and Schlessinger, J. (2010)Cell signaling by receptor tyrosine kinases. *Cell 141*, 1117–1134.

(50) Clayton, A. H., Orchard, S. G., Nice, E. C., Posner, R. G., and Burgess, A. W. (2008)Predominance of activated EGFR higher-order oligomers on the cell surface. *Growth Factors 26*, 316–324.

(51) Chung, I., Akita, R., Vandlen, R., Toomre, D., Schlessinger, J., and Mellman, I. (2010)Spatial control of EGF receptor activation by reversible dimerization on living cells. *Nature 464*, 783–787.

(52) Ariotti, N., Liang, H., Xu, Y., Zhang, Y., Yonekubo, Y., Inder, K., Du, G., Parton, R. G., Hancock, J. F., and Plowman, S. J. (2010) Epidermal growth factor receptor activation remodels the plasma membrane lipid environment to induce nanocluster formation. *Mol. Cell. Biol. 30*, 3795–3804.